Journal of Inflammation Research

Dovepress
Taylor & Francis Group

Open Access Full Text Article

ORIGINAL RESEARCH

Total Glucosides of Paeony (TGP) Inhibits Macrophages Infiltration and NLRP3-Mediated Inflammatory Response in Acute Gouty Arthritis Mice

Jing Liu[1], Ge Liu[1], Teng Chu[1], Yue Wu[1], Xingyu Yan[1], Liping Pang[2], Weirong Fang[1]

[1]School of Basic Medicine and Clinical Pharmacy, China Pharmaceutical University, Nanjing, Jiangsu, People's Republic of China; [2]Department of Medicine, Ningbo Liwah Pharmaceutical Co., Ltd, Ningbo, Zhejiang, People's Republic of China

Correspondence: Weirong Fang, School of Basic Medicine and Clinical Pharmacy, China Pharmaceutical University, Nanjing, Jiangsu, People's Republic of China, Email weirongfang@cpu.edu.cn

Purpose: The cascade of inflammation caused by the activation of NLRP3 inflammasome plays an important role in monosodium urate (MSU)-induced acute gouty arthritis (AGA) in mice. This study aimed to evaluate the therapeutic effect of total glucosides of paeony (TGP) in AGA mice and elucidate the underlying anti-inflammatory mechanism.

Materials and Methods: MSU crystals were injected into the ankle joint to establish the AGA model in mice, and bone marrow-derived macrophages (BMDMs) were primary cultured and stimulated with MSU and LPS to model inflammatory conditions in vitro. Ankle diameter was measured to quantify joint swelling. Pain was assessed by the fifty percent paw withdrawal threshold (PWT) test and the bipedal support test. Pro-inflammatory cytokine levels and arthropathological damage were analyzed by ELISA, H&E staining, and immunohistochemistry staining. The mRNA and protein expression of NLRP3 inflammasome-associated signaling pathways were determined by RT-qPCR and Western blotting, respectively. Mitochondrial oxidative damage was evaluated using flow cytometry and immunofluorescence staining.

Results: Four-week TGP administration with 360, 540, 720 mg/kg respectively significantly attenuated joint swelling and pain ($P < 0.05$, $P< 0.01$), reduced pro-inflammatory cytokine secretion ($P < 0.01$), and ameliorated joint pathology and macrophage infiltration ($P < 0.01$) in AGA mice. In BMDMs, TGP (30, 60 μg/mL) treatment notably suppressed mRNA and protein expression of NLRP3, caspase-1, and IL-1β, and lowered inflammatory factor secretion ($P < 0.05$, $P< 0.01$). Additionally, cellular and mitochondrial ROS levels were both significantly decreased ($P < 0.01$), while ATP concentration markedly increased ($P < 0.01$), suggesting improved mitochondrial function.

Conclusion: TGP significantly alleviated experimental AGA by reducing macrophage infiltration and suppressing the NLRP3-mediated inflammatory response.

Keywords: acute gouty arthritis, total glucosides of paeony, inflammatory response, NLRP3, monosodium urate, macrophage

Introduction

Acute gouty arthritis (AGA) is an inflammatory joint disorder triggered by monosodium urate (MSU) crystals deposition.[1] Clinical manifestations include localized erythema, severe pain, and joint swelling, which may progress to irreversible cartilage damage and renal impairment if inadequately managed.[2] Current pharmacotherapies—colchicine, glucocorticoids, and non-steroidal anti-inflammatory drugs (NSAIDs)—exhibit limited clinical utility due to adverse effects and poor target specificity.[3,4]

AGA pathogenesis initiates with periarticular MSU crystal deposition, stimulating macrophage activation of the NOD-like receptor family pyrin domain-containing 3 (NLRP3) inflammasome. Inflammasome assembly activates caspase-1, catalyzing maturation and secretion of interleukin (IL)-1β and other pro-inflammatory cytokines. These

Received: 12 March 2025
Accepted: 12 July 2025
Published: 29 July 2025

mediators recruit monocytes and neutrophils, amplifying the inflammatory cascade.[5,6] Reactive oxygen species (ROS) generation critically regulates NLRP3 inflammasome activation.[7]

Paeonia lactiflora Pall., documented in classical texts including Treatise on Cold Pathogenic and Miscellaneous diseases and Synopsis of Golden Chamber, possesses traditional indications for analgesia, spasmolysis, and hepatic nourishment.[8] Total glucosides of paeony (TGP), which is extracted from the plant Paeonia lactiflora Pall., exhibit favourable anti-inflammatory, analgesic, and immunomodulatory properties, with paeoniflorin (PF) identified as the primary active ingredient.[9,10] TGP has demonstrated clinical efficacy in rheumatoid arthritis and Sjögren's syndrome (SS).[8,11] Recent evidence indicates TGP suppresses NLRP3 inflammasome activation, ameliorating SS via inflammasome inhibition in submandibular glands[12] and attenuating neuroinflammation in depression models through mitochondrial protection, ROS reduction, and NLRP3 suppression.[13,14] In vitro studies by Meng et al. revealed TGP significantly inhibits MSU-induced inflammation in THP-1 macrophages via the MALAT1/miR-876-5p/NLRP3 axis, suggesting therapeutic potential for AGA.[15] However, in vivo evidence supporting TGP's efficacy in AGA remains limited.

This study investigates the therapeutic efficacy of TGP in MSU-induced AGA mice and elucidates its anti-inflammatory mechanism by suppressing NLRP3-mediated inflammatory response.

Material and Methods

Mice

One hundred and forty-four male 6–8 week old C57BL/6J mice (NO.202276910) were purchased from Jiangsu Huachuang Sino Medicine Technology Co., Ltd (Taizhou, China). All mice were maintained in SPF environment, with a temperature range of 22–24°C and a relative humidity of 40%-60%. The mice were acclimatized to the laboratory environment for a period of one week prior to the commencement of the experiment. The experimental protocols were conducted under the Guidelines for the Care and Use of Laboratory Animals of China Pharmaceutical University and were approved by the Ethics Committee (Approval No: 2022-12-023).

TGP Extraction and High Performance Liquid Chromatography (HPLC) Analysis

TGP capsules (#220319, Ningbo Liwah Pharmaceutical Co., Ltd, Ningbo, China) were prepared from the Chinese medicine Paeonia lactiflora Pall. (Bozhou, Anhui) through the following pharmaceutical process. The dried root slices underwent triple ethanol extraction using 75% (v/v) ethanol in a reflux apparatus. The filtrates were combined and concentrated to obtain an ethanolic extract, which was subsequently adjusted to neutral pH (7.0 ± 0.2) with sodium bicarbonate. Liquid-liquid extraction of the pH-adjusted solution was carried out with an ethyl acetate-n-butanol (3:1, v/v) solvent system, and a hygroscopic brown powder was obtained by vacuum concentration and lyophilization.

HPLC analysis was conducted on a Chrom core AR C18 column (4.6×250 mm, 5 μm) with a mobile phase of phosphate buffer-methanol (65:35, v/v) delivered at 1.0 mL/min. Detection was performed at 230 nm using a UV detector. The injection volume was 20 μL, and the total run time was 10 minutes per analysis.[16] 10 mg of TGP was quantitatively transferred to a 10 mL volumetric flask and dissolved in 50% (v/v) methanol, and chromatographic runs were performed on a Shimadzu LC-20AD system (Japan). The results showed that there were two major peaks, which were albiflorin and PF, respectively (Figure 1).

Formation of MSU Crystals

MSU crystals preparation made reference to the pertinent article, incorporating minor modifications.[17] A solution of uric acid sodium salt (#U2875, Sigma-Aldrich, USA) was generated by dissolving the salt (1 g) in 200 mL of 0.03 M sodium hydroxide. The pH of the solution was adjusted to 7.2 using 1 M hydrochloric acid. It was then cooled with stirring at room temperature and stored at 4°C overnight. The precipitate was filtered and subsequently dried the following day, resulting in the formation of needle-like MSU crystals. The prepared crystals were stored in a refrigerator at 4°C for future use.

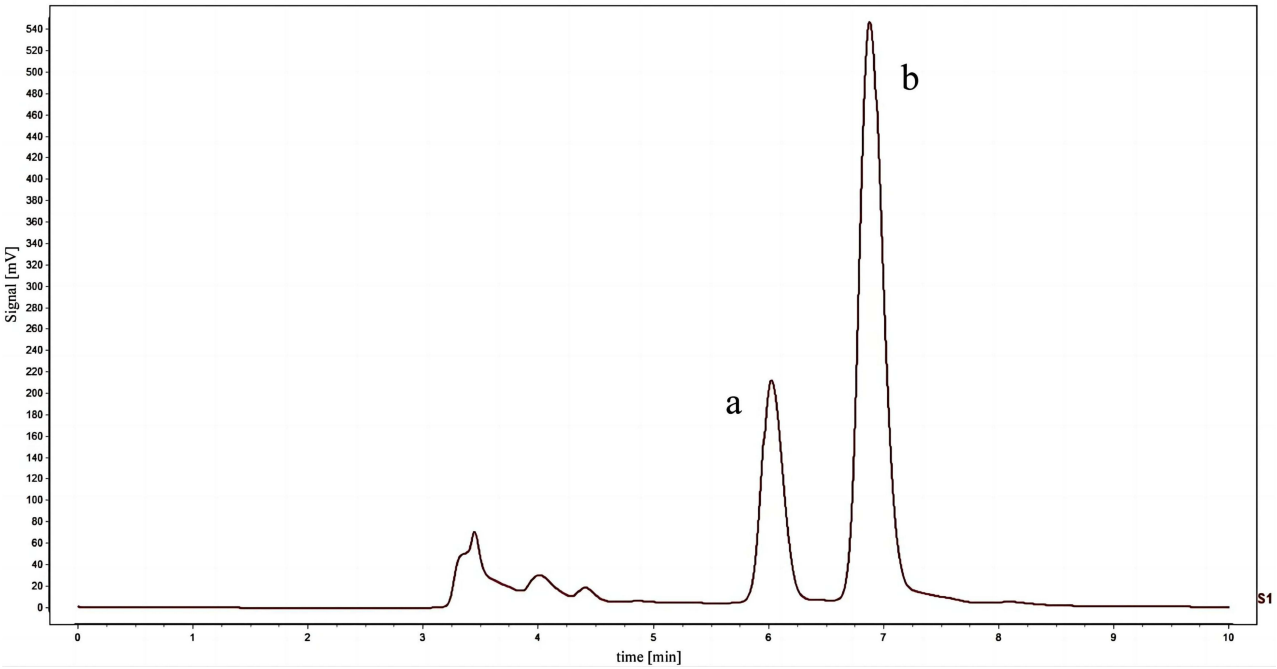

Figure 1 The HPLC chromatogram of TGP. There are two major peaks, albiflorin (**a**) and PF (**b**).

MSU-Induced AGA in Mice and TGP Treatment

The AGA model was prepared in accordance with the previously established protocol.[18] A suspension of MSU crystals in sterile saline was prepared at a concentration of 50 mg/mL. The right ankle joint was injected with 30 μL of sterile MSU suspension, and the formation of an ankle joint swelling was indicative of the success of the model. The control group was administered an equal volume of sterile saline.

Single-dose and multiple-dose were performed to evaluate the therapeutic effect of TGP against AGA, and each protocol encompassed 72 mice which were randomly allocated to six groups. Each group was given saline, Colchicine (#20220605, Guangdong Pidi Pharmaceutical Co., Ltd, Kaiping, China), and three different doses of TGP by gavage. The specific scheme is as follows.

Single-dose experiment: Mice were intragastric (i.g.) administrated with saline, Colchicine (1 mg/kg), TGP (360, 540, and 720 mg/kg) respectively immediately after MSU was injection.

Multiple-dose experiment: Mice were administrated i.g. with saline, Colchicine (0.1 mg/kg), TGP (360, 540, and 720 mg/kg) for consecutive 4 weeks. MSU was injected immediately after last administration.

Cell Culture and Stimulation

Bone marrow-derived macrophages (BMDMs) were obtained as previously described.[19] The cells were isolated from the bone marrow of mice and subsequently cultured in induction medium (comprising 10% FBS, 30% L929 cell supernatant and 60% Dulbecco's Modified Eagle Medium (DMEM, #KGL1206-500, KeyGEN BioTECH, Nanjing, China)) for 7 d.[20,21] The purity of the BMDMs was verified by flow cytometry using conjugated F4/80 and CD11b antibodies.

L929 cells were cultured in high-glucose DMEM supplemented with 10% FBS for 5 d-7 d. The cell supernatant was collected and stored at −80°C by filtration through a 0.22 μm filter. BMDMs were incubated with PF (25 μg/mL, #23180-57-6, Shanghai Stende Standard Technical Service Co., Ltd, Shanghai, China), or TGP (30 μg/mL or 60 μg/mL) for 24 h. Lipopolysaccharide (LPS, 1 μg/mL, #BS904, Biosharp, Hefei, China) was pre-treated for 1 h and stimulated with MSU (300 μg/mL) for 6 h.

https://doi.org/10.2147/JIR.S527354

Determination of Ankle Swelling

The diameters of the right ankle joints of mice in each group were measured by a specialized individual using vernier calliper at presurgical and 2, 4, 8, 12, and 24 h post-MSU injection. The ankle joint swelling was calculated according to the following formula.

Ankle joint swelling (mm) = the diameter of the ankle joint following the injection – the diameter of the ankle joint prior to the injection.

Fifty Percent Paw Withdrawal Threshold (PWT) Test

The 50% PWT in mice was determined before and 24 h after modeling using von Frey fibre filaments (Stoelting, USA), and the assay was conducted in accordance with the methodology previously described in the literature.[22]

Bipedal Support Test

Following a 24-hour period of MSU injection, the mice were placed within a single channel of the YLS-11A channel mouse foot support force measuring instrument (Zhongshi Science&Technology, Beijing, China) and subjected to a 60° climbing experiment. The difference in support force between the left and right hind legs of the mice while standing was recorded.

H&E and Immunohistochemistry Staining

The right ankle joint tissue of mice was fixed in 4% paraformaldehyde (#22097198, Biosharp, Hefei, China), decalcified after 72 h of fixation, dehydrated in gradient alcohol, embedded in paraffin, and sectioned. The paraffin sections were deparaffinised, stained with hematoxylin for 15 min, stained with 0.5% eosin solution for 3 min, and rinsed with double-distilled water. The sections were sealed with neutral gum and observed under the microscope. The pathological features of ankle joint are synovial edema, vascular injury and inflammatory cell infiltration.

The above paraffin sections were deparaffinized in xylene and subsequently rehydrated with varying concentrations of ethanol. The sections were incubated with the primary antibody (anti-F4/80 monoclonal antibody (#29414-1-AP, Proteintech, Wuhan, China)) overnight at 4°C. They were then washed with PBS and incubated with the enzyme-labelled secondary antibody for 20 min. Staining was performed using a freshly prepared DAB solution and counter-stained with haematoxylin. The sections were observed under a microscope and the rate of positive cells in the field of view was analyzed using ImageJ.

ELISA Assay

The concentrations of IL-1β (#ml098416), IL-6 (#ml063159), IL-8 (#ml063162), IL-18 (#ml002294) and TNF-α (#ml002098) in serum and cell culture supernatants were determined using ELISA kits (Shanghai Enzyme-linked Biotechnology Co., Ltd, Shanghai, China).

ATP Content Assay

ATP content was measured with the Enhanced ATP Assay Kit (#S0027, Beyotime, Shanghai, China) in accordance with the manufacturer's instructions.

Reverse Transcription Quantitative Real-Time PCR (RT-qPCR)

Total RNA was extracted from BMDMs using the Trizol method. cDNA was reverse-transcribed from RNA using HiScript II Reverse Transcriptase Reagent (#R223, Vazyme, Nanjing, China). Amplification reactions were carried out by gene-specific primers (Table 1) from GENEWIZ (Suzhou, China). The mRNA levels of the target genes were quantified using SYBR Master Mix (#Q331, Vazyme, Nanjing, China) and the $2^{-\Delta\Delta Ct}$ method, with β-actin serving as the internal reference.

Western Blotting

The cells were lysed with RIPA buffer, supplemented with PMSF, and the protein concentration was determined using the BCA method. Equal aliquots of protein were subjected to 10%-15% sodium dodecyl sulfate-polyacrylamide gel

Table 1 Gene-Specific Primer Sequences

Genes	Primer Sequences (5′ to 3′)
β-actin	F: GGCTGTATTCCCCTCCATCG
	R: CCAGTTGGTAACAATGCCATGT
NLRP3	F: ATTACCCGCCCGAGAAAGG
	R: TCGCAGCAAAGATCCACACAG
Caspase-1	F: ACAAGGCACGGGACCTATG
	R: TCCCAGTCAGTCCTGGAAATG
IL-1β	F: GCAACTGTTCCTGAACTCAACT
	R: ATCTTTTGGGGTCCGTCAACT

electrophoresis (SDS-PAGE) and subsequently transferred to a 0.45 μm PVDF membrane. The strips were incubated with rapid containment solution for 10 min at room temperature, after which incubation of primary antibodies (anti-NLRP3 (1:1000, #YT5382, Immunoway, USA), anti-Caspase-1 (1:1000, #YT5743, Immunoway, USA), anti-IL-1β (1:1000, #ab254360, Abcam, USA), anti-pro-IL-1β (1:1000, #WL02257, Wanleibio, Shenyang, China), and anti-β-actin (1:1000, #AC038, ABclonal, Wuhan, China)) was undertaken overnight at 4°C. TBST washes were performed on three occasions, then the samples were incubated with peroxidase-coupled goat anti-rabbit IgG (1:100,000, #HA1001, HuaBio, Hangzhou, China) for 1 h. Finally, the protein bands are visualized within the imaging system utilising SuperKine™ Ultrasensitive ECL Luminescent Solution (#BMU102, Abbkine, Wuhan, China). Quantitative analysis was conducted using the ImageJ software, with the target protein to β-actin ratio serving as an indicator of protein expression levels.

Intracellular and Mitochondrial ROS Detection

Intracellular ROS were measured using the Reactive Oxygen Detection Kit (#S0033S, Beyotime, Shanghai, China). Cells were inoculated in 6-well plates and treated with the fluorescent probe dichloro-dihydrofluorescein diacetate (DCFH-DA) for 30 min, whereupon a further detection step was performed using flow cytometry.

MitoSOX Red (#BB-441152, BestBio, Shanghai, China), Mito-Tracker Green (#C1048, Beyotime, Shanghai, China) and Hoechst 33342 (#C1022, Beyotime, Shanghai, China) were co-stained in order to label mitochondrial ROS. The resulting cell images were then observed via the utilization of fluorescence microscopy.

Statistical Analysis

All data were presented as mean ± standard error of the mean (SEM). Statistical analyses were performed using SPSS 27.0, and one-way analysis of variance (ANOVA) was used to test for differences between groups. Normality and homogeneity of variance were assessed with the Shapiro–Wilk test and Levene's test (both at α=0.05). When homogeneity of variance was confirmed, the LSD test was selected; otherwise, the Games-Howell test was employed. $p < 0.05$ was regarded as statistically significant.

Results

Only 720 mg/kg TGP with Single-Dose Relieves Pain and Swelling in AGA Mice

Pain and joint swelling constitute the hallmark clinical manifestations of gout flares. Joint swelling was indicated by the diameter of the ankle. The results demonstrated that the swelling index peaked at 12 h following MSU injection, at which time all TGP dosage regimens significantly attenuated this phenomenon (Figure 2A). Only the high-dose TGP (720 mg/kg) group showed a marked reduction in ankle swelling at 24 h post-injection in comparison with the vehicle group (Figure 2A). Pain is another feature that responds to the severity of AGA. The 50% PWT obtained by using the up and down method is widely regarded as the gold standard for the assessment of mechanical pain, and thresholds are inversely proportional to pain intensity. No significant threshold improvements were observed in any treatment group at 24 h post-induction (Figure 2B). The test of the bipedal support provided complementary pain assessment, effectively controlling

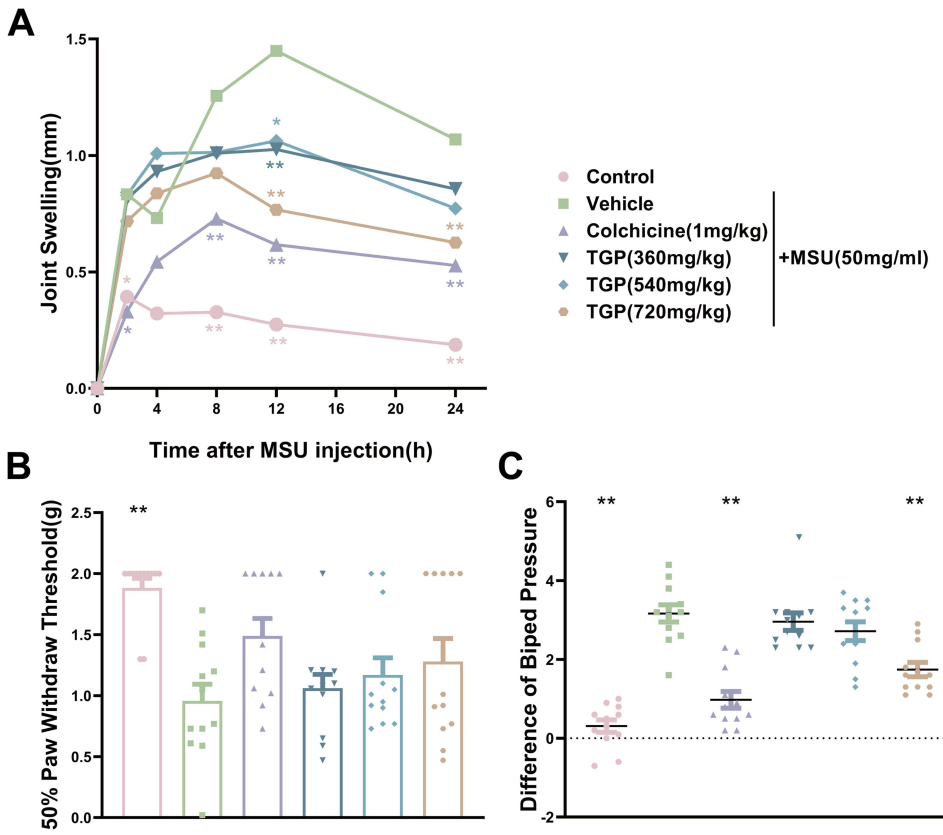

Figure 2 Effect of a single-dose administration of TGP on MSU-induced AGA in mice. (**A**) Changes in ankle swelling at different time points after MSU injection; (**B** and **C**) Mechanical pain threshold and difference in bipedal support were determined in each group of mice at 24 h post-MSU injection. Data are expressed as mean ± SEM, n = 12. *P < 0.05, **P < 0.01 vs Vehicle group.

for confounding behavioral factors like anxiety to accurately reflect analgesic efficacy. The difference was considerably higher in the vehicle group of mice but was only reduced by TGP (720 mg/kg) (Figure 2C). The above results demonstrated that only a single dose of 720 mg/kg TGP relieved pain and swelling in AGA mice.

Multiple-Dose of TGP Remarkably Alleviates Pathological Symptoms of AGA Mice

As shown in Figure 3, four-week intragastric administration of TGP (360, 540, and 720 mg/kg) significantly attenuated ankle swelling and reduced the difference of bipedal support relative to the vehicle group (Figure 3A and C). Subsequently, TGP treatment resulted in a pronounced enhancement of the pain threshold (Figure 3B). Histopathological analysis via H&E staining confirmed TGP-mediated mitigation of ankle joint pathology, effectively ameliorating MSU-induced synovial edema, vasodilation, and inflammatory cell infiltration (Figure 3D). Based on these findings, the multiple-dose TGP regimen was employed in subsequent in vivo experiments.

TGP Treatment Suppresses Systemic Inflammatory Responses and Reduces Macrophages Infiltration

Serum inflammatory factor levels in mice were measured by ELISA. Pro-inflammatory factor, TNF-α, was significantly decreased following TGP treatment (Figure 4A). Inflammatory cytokines associated with NLRP3 inflammasome activation (IL-1β, IL-6, IL-8, and IL-18) were elevated post-MSU injection. All TGP dosages reduced these cytokine levels (Figure 4B–E). Furthermore, MSU stimulation induced substantial macrophage infiltration in the joint during the acute phase, as evidenced by increased F4/80-positive cells. This infiltration was attenuated by TGP administration at 540 or 720 mg/kg (Figure 5A and B).

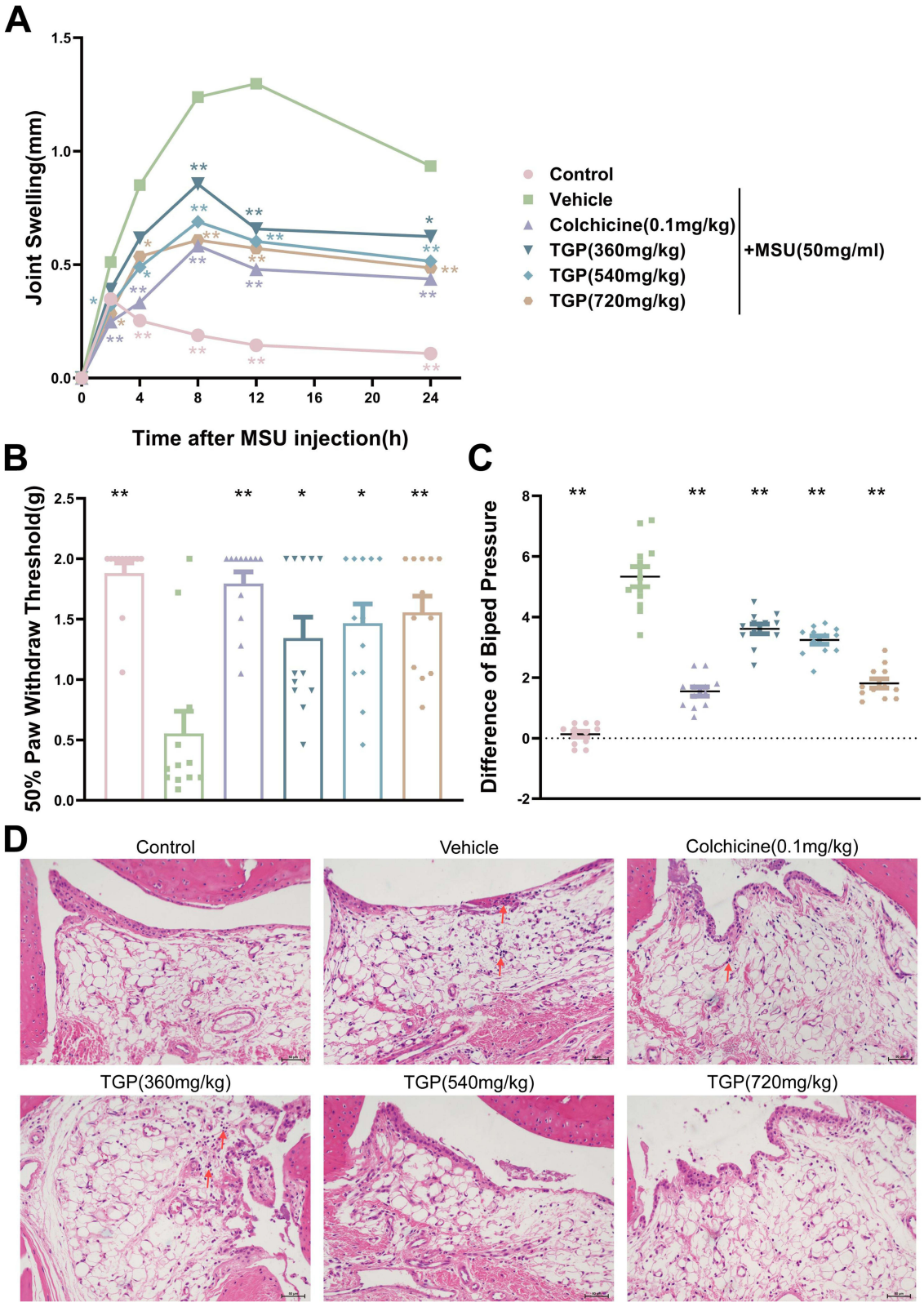

Figure 3 Multiple-dose of TGP administration effectively alleviates MSU-induced AGA in mice. (**A**) Changes in ankle joint swelling at different time points after MSU injection; (**B** and **C**) Mechanical pain threshold and difference in bipedal support were measured in each group of mice at 24 h after MSU injection; (**D**) Representative H&E staining images of ankle joints, and arrows indicate infiltrating inflammatory cells. Data are shown as mean ± SEM, n = 12. *P < 0.05, **P < 0.01 vs Vehicle group.

https://doi.org/10.2147/JIR.S527354

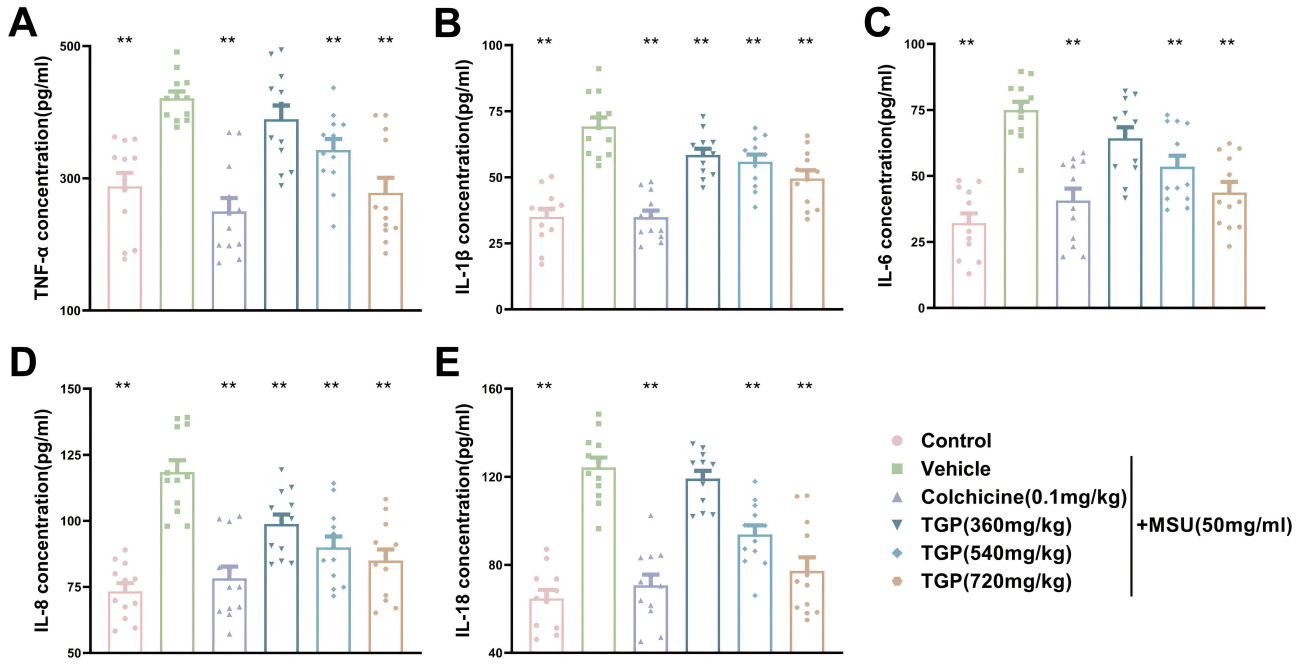

Figure 4 TGP suppresses systemic inflammatory responses in mice. (**A**–**E**) ELISA was performed to detect serum TNF-α, IL-1β, IL-6, IL-8 and IL-18 contents (n = 12). Data are expressed as mean ± SEM. **P < 0.01 vs Vehicle group.

TGP Reduces IL-1β Production and NLRP3 Inflammasome Activation in MSU+LPS Stimulated BMDMs

Numerous studies have shown that the inflammatory response in gout can be attributed to the activation of NLRP3 inflammasome and the subsequent secretion of IL-1β.[23,24] RT-qPCR and Western blotting analysis showed that incubation with TGP notably suppressed the IL-1β, NLRP3, and caspase-1 mRNA expression (Figure 6A–C), and IL-1β, pro-IL-1β, NLRP3, caspase-1, and cleaved caspase-1 proteins expression (Figure 7A–F). TNF-α, IL-1β, and IL-18 secretion after MSU+LPS stimulation were found to be significantly elevated in comparison to untreated cells, as determined by ELISA. Furthermore, these levels declined substantially following treatment with TGP (Figure 6D–F).

TGP Alleviates Mitochondrial Dysfunction and ROS Generation in MSU+LPS Stimulated BMDMs

ROS was an upstream signal of NLRP3 inflammasomes, which could be detected by flow cytometry using DCFH-DA staining in live cells. Stimulation with MSU+LPS significantly increased intracellular ROS production (52.8%), which was significantly inhibited by TGP (41.2% and 25.2%; Figure 8A and B). Furthermore, mitochondrial ROS and mitochondria were labeled using MitoSOX Red and MitoTracker Green, respectively. MSU+LPS stimulation markedly elevated fluorescence intensity, indicating mitochondrial oxidative stress, while TGP incubation significantly suppressed this response and attenuated mitochondrial dysfunction (Figure 8C and D). Consistent with mitochondrial damage, ATP levels decreased substantially post-MSU+LPS stimulation but were restored by TGP treatment (Figure 8E).

Discussion

In this study, TGP with multiple-dose demonstrated efficacy in reducing ankle joint swelling and pain in AGA mice, while attenuating histopathological damage. Furthermore, a substantial reduction in the serum levels of inflammatory factors TNF-α, IL-1β, IL-6, IL-8, and IL-18 was observed, along with the inhibition of macrophage infiltration. Mechanistically, TGP suppressed NLRP3 inflammasome activation by decreasing ROS production and ameliorating mitochondrial dysfunction, thereby reducing expression and secretion of NLRP3, caspase-1, and IL-1β.

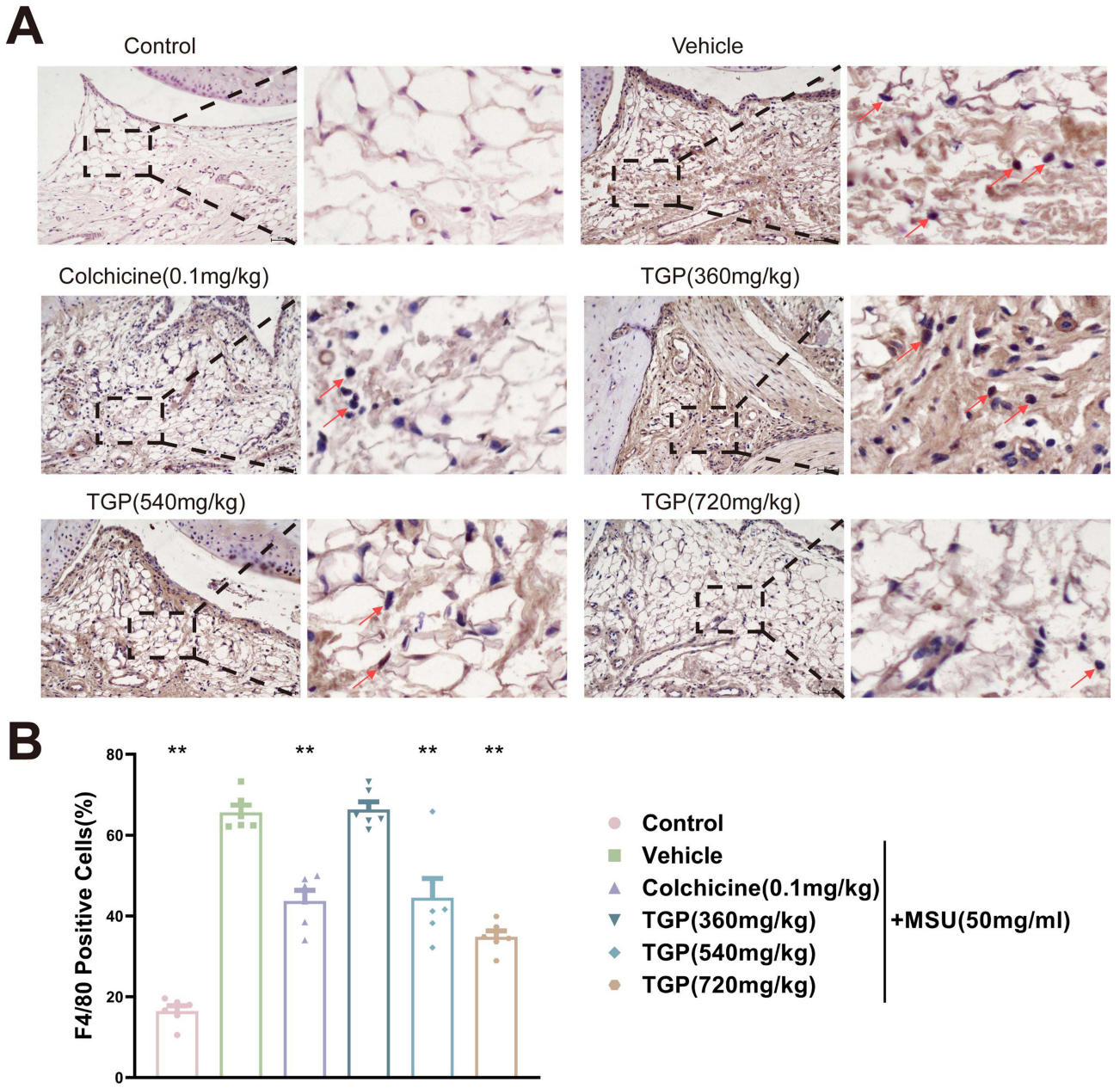

Figure 5 TGP reduces local inflammation in mice. **(A)** Representative image of immunohistochemical staining, arrows indicate F4/80-positive cells; (**B**) Statistical analysis of F4/80 positive cells (n = 6). Data are expressed as mean ± SEM. **P < 0.01 vs Vehicle group.

TGP has been clinically approved for the treatment of immunological diseases such as rheumatoid arthritis due to its anti-inflammatory, analgesic, and immunomodulatory effects.[9,11] However, its therapeutic potential in gout remains incompletely characterized. Gout flares manifest from excessive MSU deposition, triggering intra-articular inflammation. Consistent with this pathogenesis, MSU injections induced acute inflammatory reactions in our model. TGP with multiple-dose was more effective than single-dose in the treatment of AGA mice as our results indicate may related to the pharmacological characteristic of TGP. The immunomodulatory effects of TGP on immune cells (including macrophages, Th17 cells, Treg, and dendritic cells) require cumulative exposure for full activation.[25,26] Long-term administration of TGP has been utilized in studies pertaining to its treatment of rheumatoid arthritis, lupus nephritis, and SS.[27,28] Notably, while multiple studies employ 8-week regimens, evidence indicates significant efficacy after 4-week treatment. Considering clinical compliance and experimental feasibility, we implemented a 4-week intervention.[12,29] As anticipated,

https://doi.org/10.2147/JIR.S527354

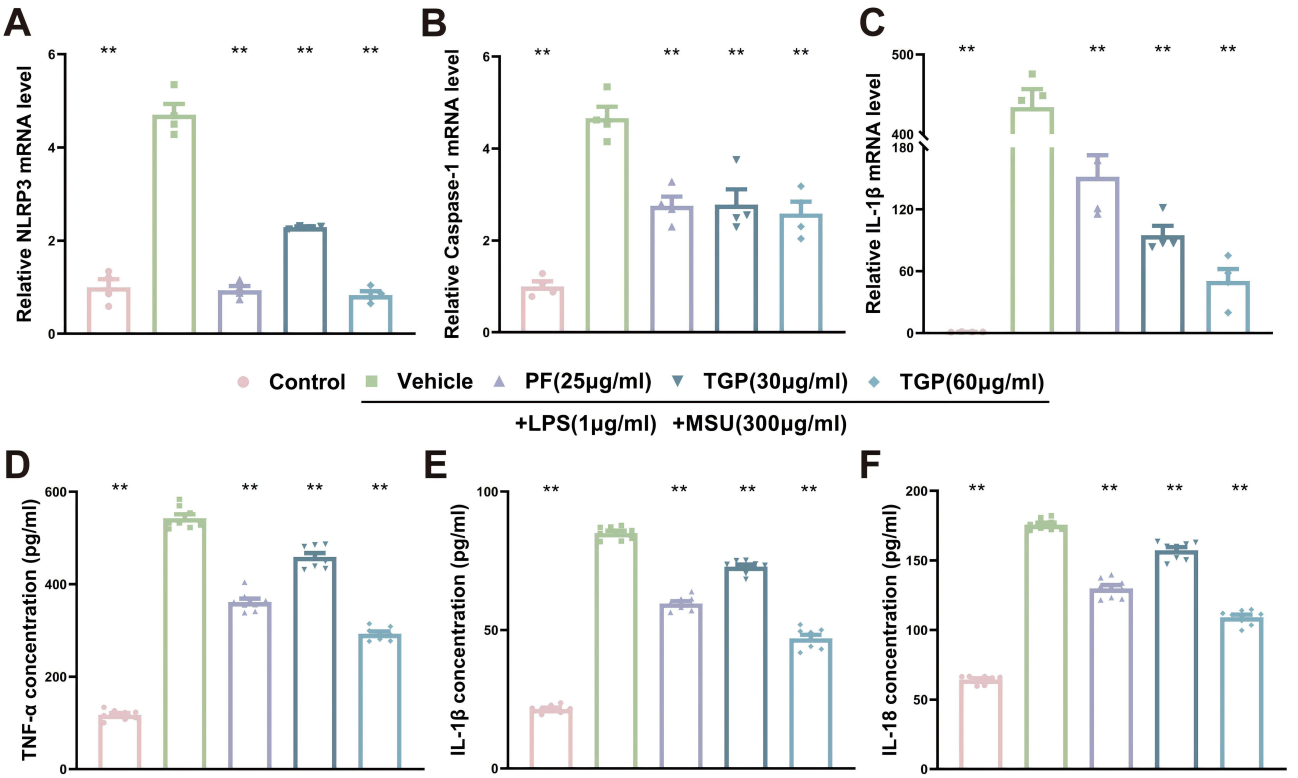

Figure 6 TGP reduces IL-1β production and NLRP3 inflammasome activation in MSU+LPS stimulated BMDMs. BMDMs were treated with or without TGP or PF for 24 h, then stimulated with LPS (1 μg/mL) for 1 h and MSU (300 μg/mL) for 6 h. (**A**– **C**) The mRNA levels of IL-1β, NLRP3, and caspase-1 were analyzed by RT-qPCR (n = 4); (**D–F**) ELISA was performed to detect the levels of secreted TNF-α, IL-1β and IL-18 in the cell culture supernatant (n = 6). Data are expressed as mean ± SEM. **P < 0.01 vs Vehicle group.

ankle swelling was obviously reduced in AGA mice after TGP multiple-dose treatment. A decrease in the difference of bipedal support and an increase in 50% PWT indicated a significant reduction in pain in mice. Histopathological amelioration of joint damage, decreased inflammatory cell infiltration, and reduced serum inflammatory cytokine levels further substantiate TGP's efficacy against AGA.

Macrophages play an important role in the initiation of gout inflammation. The prevailing perspective suggests that gout flares commence with MSU-induced NLRP3 inflammasome activation in macrophages, triggering downstream inflammatory cascades.[30] Immunohistochemistry revealed substantial macrophage infiltration in joints post-MSU stimulation, which was significantly attenuated by TGP treatment, indicating macrophage-mediated anti-inflammatory effects. For subsequent in vitro experiments, BMDMs were selected due to their phenotypic relevance to murine physiology. MSU synergizes with LPS to nucleate the NLRP3 inflammasome complex, activating caspase-1. This protease catalyzes cleavage of pro-IL-1β and pro-IL-18 into mature effector cytokines, enabling extracellular secretion and inflammatory amplification.[31,32] TGP treatment significantly suppressed NLRP3 and caspase-1 expression at mRNA and protein levels, inhibiting inflammasome activation. Consequently, TNF-α, IL-1β, and IL-18 secretion diminished, markedly attenuating the inflammatory response.

ROS primarily originate from mitochondrial oxidative phosphorylation. Under physiological conditions, ROS serve as essential defense molecules against pathogens. However, external stimuli can significantly increase ROS production.[33] High concentrations of ROS induce oxidative stress, causing macromolecular damage and contributing to pathologies including malignancies and arthritis.[34] It has been previously reported that ROS production is an important upstream signal for activation of NLRP3 inflammasomes.[7,35,36] We found that MSU stimulation caused cells to undergo oxidative stress, and TGP treatment effectively inhibited intracellular and mitochondrial ROS production to exert antioxidant effects. Excessive ROS promote mitochondrial dysfunction through respiratory chain inhibition and impaired energy metabolism.[37] TGP administration restored diminished ATP levels, indicating partial recovery of mitochondrial function.

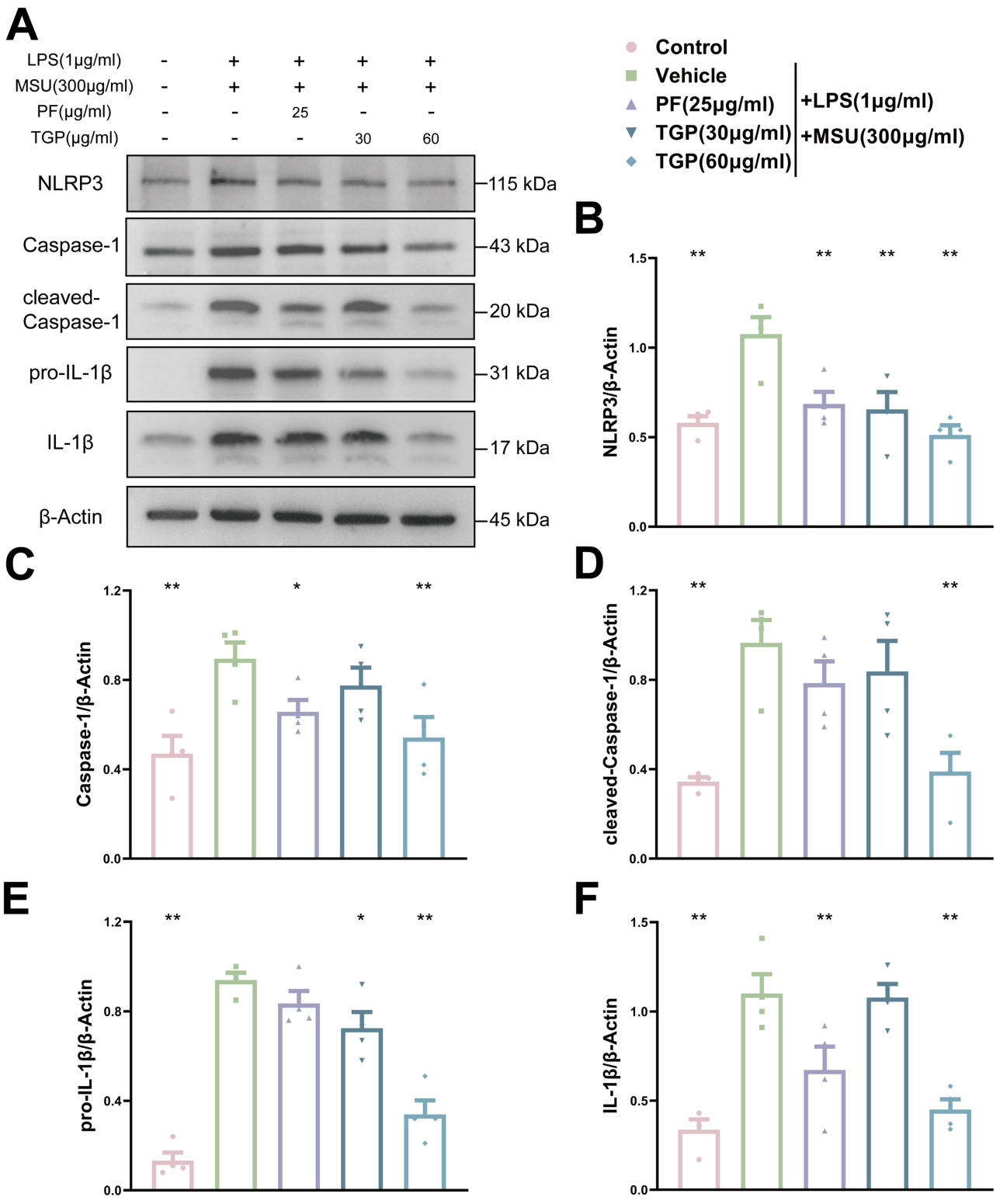

Figure 7 TGP suppresses expression of key NLRP3 inflammasome components. BMDMs were treated with or without TGP or PF for 24 h, then stimulated with LPS (1 μg/mL) for 1 h and MSU (300 μg/mL) for 6 h. (**A**–**F**) Western blotting was used to determine the NLRP3, caspase-1, cleaved caspase-1, IL-1β, and pro-IL-1β protein expression levels. Data are expressed as mean ± SEM, n = 4. *P < 0.05, **P < 0.01 vs Vehicle group.

Collectively, our results establish that TGP modulates ROS production to regulate NLRP3-mediated anti-inflammatory responses. This finding parallels the mechanism reported by Wang et al. wherein tetrahydropalmatine alleviates gout by suppressing ROS-mediated NLRP3 inflammasome activation.[38] However, our investigation extended beyond

https://doi.org/10.2147/JIR.S527354

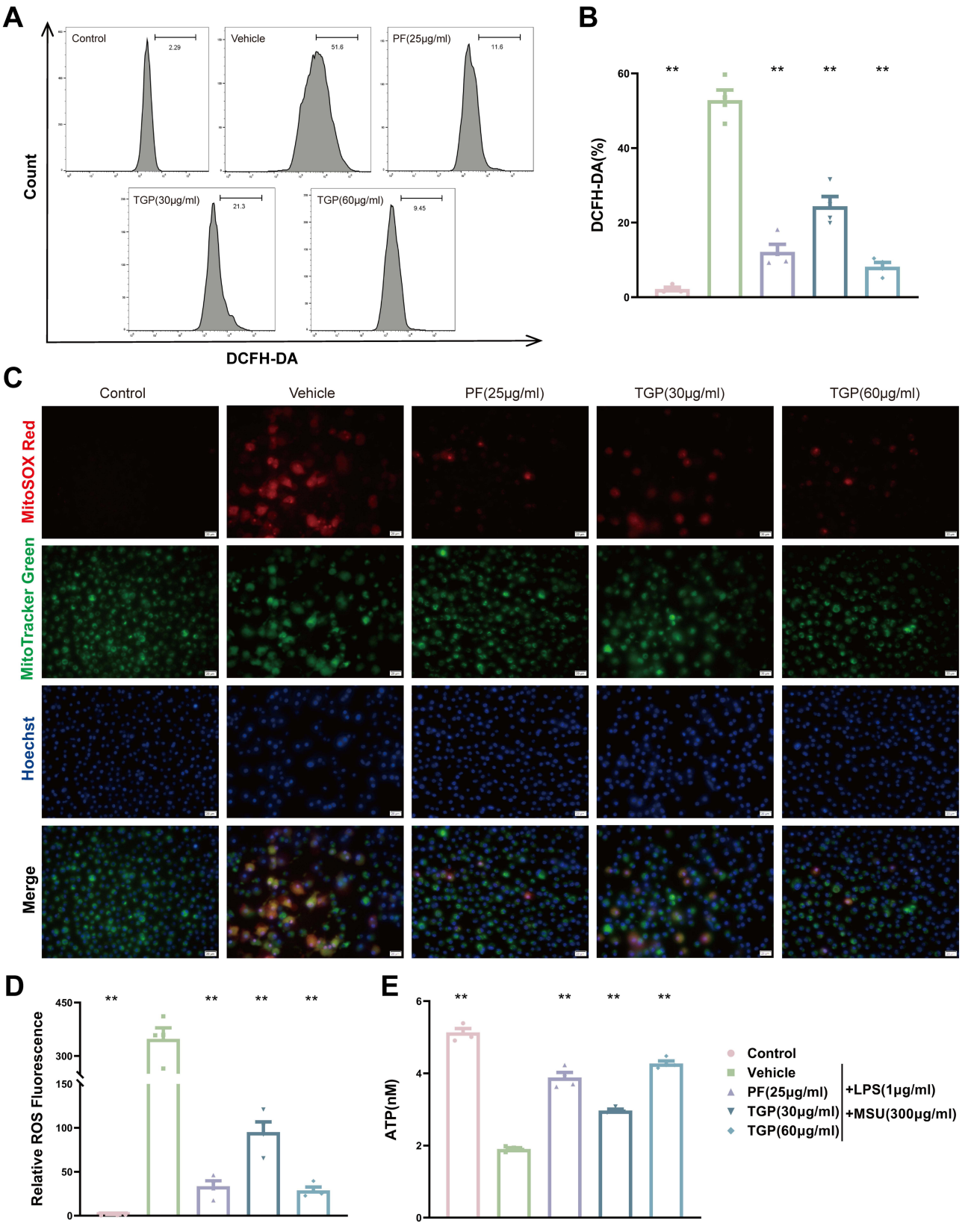

Figure 8 TGP alleviates mitochondrial dysfunction and ROS production in MSU+LPS stimulated BMDMs. BMDMs were treated with or without TGP or PF for 24 h, then stimulated with LPS (1 μg/mL) for 1 h and MSU (300 μg/mL) for 6 h. (**A** and **B**) Flow cytometry detection of DCFH-DA to assess intracellular ROS levels; (**C** and **D**) For analysis of mitochondrial ROS, cells were stained with MitoSOX Red and MitoTracker Green, and fluorescence images were obtained by fluorescence microscopy and analyzed by Image J; (**E**) The ATP content was read using fluorescence microplate reader. Data are expressed as mean ± SEM, n = 4. **P < 0.01 vs Vehicle group.

intracellular ROS quantification to specifically focus on mtROS as a pivotal mediator. We established a direct correlation between ROS suppression and restoration of mitochondrial function, thereby providing compelling experimental evidence for TGP's mitochondrial protection and attenuation of oxidative stress damage. In contrast, Jiang et al. demonstrated that PF, an active constituent of TGP, inhibits NLRP3 inflammasome activation in submandibular glands of SS mice through modulation of the Nrf2/HO-1 axis.[39] While this offers valuable insights into TGP's mechanism in SS, it does not address the interplay among ROS, energy metabolism, and inflammasome activation.

Collectively, this study systematically elucidates the therapeutic effect of TGP in AGA model by suppressing macrophage infiltration and NLRP3-mediated inflammatory response, while further revealing its protective role in mitochondrial function. These findings not only extend our understanding of TGP's anti-inflammatory mechanisms but also establish a solid experimental foundation for its clinical application in AGA management. There are some limitations in current research. Firstly, in vitro findings could not be validated in vivo due to decalcification and fixation protocols applied to murine ankle joints post-resection, which precluded assessment of ROS and NLRP3 inflammasome activation markers. Secondly, the diverse and complex composition of TGP prevented analysis of individual monomer contributions. Additionally, the mechanism study was not in-depth enough, and further exploration of the epigenetic regulation is on going in our lab.

Conclusion

In summary, TGP exerts therapeutic effects on AGA mice by reducing macrophage infiltration and suppressing the NLRP3-mediated inflammatory response.

Abbreviations

NLRP3, NOD-like receptor family pyrin domain containing 3; MSU, monosodium urate; AGA, acute gouty arthritis; TGP, total glucosides of paeony; SS, Sjögren's syndrome; HPLC, high performance liquid chromatography; BMDMs, bone marrow-derived macrophages; LPS, lipopolysaccharide; PWT, paw withdrawal threshold; IL, interleukin; ROS, reactive oxygen species; NSAIDs, nonsteroidal anti-inflammatory drugs; PF, paeoniflorin; DMEM, Dulbecco's Modified Eagle Medium; SDS-PAGE, sodium dodecyl sulfate-polyacrylamide gel electrophoresis; DCFH-DA, dichloro-dihydrofluorescein diacetate; SEM, standard error of the mean; ANOVA, analysis of variance.

Ethics Approval and Informed Consent

The experimental protocols of this study were conducted under the Guidelines for the Care and Use of Laboratory Animals of China Pharmaceutical University and were approved by the Ethics Committee (Approval No: 2022-12-023).

Consent for Publication

All authors approved the publication of this manuscript.

Acknowledgments

We sincerely appreciate all participants for their invaluable contributions to this study. We are grateful to China Pharmaceutical University for providing advanced instrumentation and laboratory facilities, as well as to Ningbo Lihua Pharmaceutical Co., Ltd. for technical and financial support. Finally, we acknowledge the dedication of all researchers who participated in data collection and analysis throughout this project. The successful completion of this study could not have been achieved without the collective efforts of every individual involved.

Author Contributions

All authors made a significant contribution to the work reported, whether that is in the conception, study design, execution, acquisition of data, analysis and interpretation, or in all these areas; took part in drafting, revising or critically reviewing the article; gave final approval of the version to be published; have agreed on the journal to which the article has been submitted; and agree to be accountable for all aspects of the work.

Funding

This work was supported by National Natural Science Foundation of China [grant number 82174051] and Ningbo Key Research and Development Program [2023Z205].

Disclosure

The authors report no conflicts of interest in this work.

References

1. Dalbeth N, Gosling AL, Gaffo A, Abhishek A. Gout. *Lancet*. 2021;397(10287):1843–1855. doi:10.1016/S0140-6736(21)00569-9
2. Bodofsky S, Merriman TR, Thomas TJ, Schlesinger N. Advances in our understanding of gout as an auto-inflammatory disease. *Semin Arthritis Rheumatism*. 2020;50(5):1089–1100. doi:10.1016/j.semarthrit.2020.06.015
3. Shi C, Zhou Z, Chi X, et al. Recent advances in gout drugs. *Eur J Med Chem*. 2023;245(Pt 1):114890. doi:10.1016/j.ejmech.2022.114890
4. Peng X, Li X, Xie B, et al. Gout therapeutics and drug delivery. *J Control Rel*. 2023;362:728–754. doi:10.1016/j.jconrel.2023.09.011
5. Martin WJ, Walton M, Harper J. Resident macrophages initiating and driving inflammation in a monosodium urate monohydrate crystal-induced murine peritoneal model of acute gout. *Arthritis Rheum*. 2009;60(1):281–289. doi:10.1002/art.24185
6. Wang S, Liu W, Wei B, et al. Traditional herbal medicine: therapeutic potential in acute gouty arthritis. *J Ethnopharmacol*. 2024;330:118182. doi:10.1016/j.jep.2024.118182
7. Wu H, Wang Y, Huang J, Li Y, Lin Z, Zhang B. Rutin ameliorates gout via reducing XOD activity, inhibiting ROS production and NLRP3 inflammasome activation in quail. *Biomed Pharmacothe*. 2023;158:114175. doi:10.1016/j.biopha.2022.114175
8. Zhang L, Wei W. Anti-inflammatory and immunoregulatory effects of paeoniflorin and total glucosides of paeony. *Pharmacol Ther*. 2020;207:107452. doi:10.1016/j.pharmthera.2019.107452
9. Luo J, Jin DE, Yang GY, et al. Total glucosides of paeony for rheumatoid arthritis: a systematic review of randomized controlled trials. *Complementary Ther Med*. 2017;34:46–56. doi:10.1016/j.ctim.2017.07.010
10. Liu B, Meng X, Ma Y, et al. Clinical safety of total glucosides of paeony adjuvant therapy for rheumatoid arthritis treatment: a systematic review and meta-analysis. *BMC Complement Med Therap*. 2021;21(1):102. doi:10.1186/s12906-021-03252-y
11. Jiang H, Li J, Wang L, et al. Total glucosides of paeony: a review of its phytochemistry, role in autoimmune diseases, and mechanisms of action. *J Ethnopharmacol*. 2020;258:112913. doi:10.1016/j.jep.2020.112913
12. Jiang T, Guo J, Wang Y, et al. Total glucosides of paeony alleviates experimental Sjögren's syndrome through inhibiting NLRP3 inflammasome activation of submandibular gland cells. *Clin Experiment Rheumatol*. 2023;41(12):2502–2510. doi:10.55563/clinexprheumatol/7kbuok
13. Su L, Lu H, Zhang D, et al. Total paeony glycoside relieves neuroinflammation to exert antidepressant effect via the interplay between NLRP3 inflammasome, pyroptosis and autophagy. *Phytomedicine*. 2024;128:155519. doi:10.1016/j.phymed.2024.155519
14. Wang X, Su L, Liu S, et al. Paeoniflorin Inhibits the Activation of Microglia and Alleviates Depressive Behavior by Regulating SIRT1-NF-kB-NLRP3/Pyroptosis Pathway. *Int J Mol Sci*. 2024;25(23):12543. doi:10.3390/ijms252312543
15. Meng Q, Meng W, Bian H, et al. Total glucosides of paeony protects THP-1 macrophages against monosodium urate-induced inflammation via MALAT1/miR-876-5p/NLRP3 signaling cascade in gouty arthritis. *Biomed Pharmacothe*. 2021;138:111413. doi:10.1016/j.biopha.2021.111413
16. Liu G, Wang J, Liu J, et al. Total glucosides of paeony alleviates Sjogren's syndrome by inhibiting Th1 and Th17 responses. *Phytomedicine*. 2025;139:156525. doi:10.1016/j.phymed.2025.156525
17. Fattori V, Zarpelon AC, Staurengo-Ferrari L, et al. Budlein A, a Sesquiterpene Lactone From Viguiera robusta, Alleviates Pain and Inflammation in a Model of Acute Gout Arthritis in Mice. *Front Pharmacol*. 2018;9:1076. doi:10.3389/fphar.2018.01076
18. Reber LL, Marichal T, Sokolove J, et al. Contribution of mast cell-derived interleukin-1β to uric acid crystal-induced acute arthritis in mice. *Arthritis Rheumatol*. 2014;66(10):2881–2891. doi:10.1002/art.38747
19. Ying W, Cheruku PS, Bazer FW, Safe SH, Zhou B. Investigation of macrophage polarization using bone marrow derived macrophages. *JoVE*. 2013;(76). doi:10.3791/50323-v.
20. Boltz-Nitulescu G, Wiltschke C, Holzinger C, et al. Differentiation of rat bone marrow cells into macrophages under the influence of mouse L929 cell supernatant. *J Leukoc Biol*. 1987;41(1):83–91. doi:10.1002/jlb.41.1.83
21. Simkin J, Aloysius A, Adam M, et al. Tissue-resident macrophages specifically express Lactotransferrin and Vegfc during ear pinna regeneration in spiny mice. *Dev Cell*. 2024;59(4):496–516.e6. doi:10.1016/j.devcel.2023.12.017
22. Mills C, Leblond D, Joshi S, et al. Estimating efficacy and drug ED50's using von Frey thresholds: impact of weber's law and log transformation. *J Pain*. 2012;13(6):519–523. doi:10.1016/j.jpain.2012.02.009
23. So AK, Martinon F. Inflammation in gout: mechanisms and therapeutic targets. *Nat Rev Rheumatol*. 2017;13(11):639–647. doi:10.1038/nrrheum.2017.155
24. Yin C, Liu B, Wang P, et al. Eucalyptol alleviates inflammation and pain responses in a mouse model of gout arthritis. *Br J Pharmacol*. 2020;177(9):2042–2057. doi:10.1111/bph.14967
25. Wang K, Wu YG, Su J, Jj Z, Zhang P, Qi XM. Total glucosides of paeony regulates JAK2/STAT3 activation and macrophage proliferation in diabetic rat kidneys. *Am J Chin Med*. 2012;40(3):521–536. doi:10.1142/S0192415X12500401
26. Sun Y, Liu T, Zhao X. Progress in the Study of Chemical Structure and Pharmacological Effects of Total Paeony Glycosides Isolated from Radix Paeoniae Rubra. *Curr Issues Mol Biol*. 2024;46(9):10065–10086. doi:10.3390/cimb46090601
27. Li B, Liu G, Liu R, et al. Total glucosides of paeony (TGP) alleviates Sjogren's syndrome through inhibiting inflammatory responses in mice. *Phytomedicine*. 2020;71:153203. doi:10.1016/j.phymed.2020.153203
28. Liang CL, Jiang H, Feng W, et al. Total Glucosides of Paeony Ameliorate Pristane-Induced Lupus Nephritis by Inducing PD-1 ligands(+) Macrophages via Activating IL-4/STAT6/PD-L2 Signaling. *Front Immunol*. 2021;12:683249. doi:10.3389/fimmu.2021.683249

29. Liao T, Kang J, Ma Z, et al. Total glucosides of white paeony capsule alleviate articular cartilage degeneration and aberrant subchondral bone remodeling in knee osteoarthritis. *Phytother Res*. 2025;39(4):1758–1775. doi:10.1002/ptr.8210
30. Tan H, Zhang S, Liao J, et al. Mechanism of macrophages in gout: recent progress and perspective. *Heliyon*. 2024;10(19):e38288. doi:10.1016/j.heliyon.2024.e38288
31. Fu J, Wu H. Structural Mechanisms of NLRP3 Inflammasome Assembly and Activation. *Annu Rev Immunol*. 2023;41(1):301–316. doi:10.1146/annurev-immunol-081022-021207
32. Liu J, Liu G, Chu T, Wu Y, Yang LZ, Fang W. The Progress of Immune Cells-induced Inflammatory Response in Gout. *Curr Pharm Des*. 2025;31(31):2465–2480. doi:10.2174/0113816128369016250306050522
33. Liu J, Han X, Zhang T, Tian K, Li Z, Luo F. Reactive oxygen species (ROS) scavenging biomaterials for anti-inflammatory diseases: from mechanism to therapy. *J Hematol Oncol*. 2023;16(1):116. doi:10.1186/s13045-023-01512-7
34. Cheung EC, Vousden KH. The role of ROS in tumour development and progression. *Nat Rev Cancer*. 2022;22(5):280–297. doi:10.1038/s41568-021-00435-0
35. Lin Y, Luo T, Weng A, et al. Gallic Acid Alleviates Gouty Arthritis by Inhibiting NLRP3 Inflammasome Activation and Pyroptosis Through Enhancing Nrf2 Signaling. *Front Immunol*. 2020;11:580593. doi:10.3389/fimmu.2020.580593
36. Wei H, Liu B, Yin C, et al. Electroacupuncture improves gout arthritis pain via attenuating ROS-mediated NLRP3 inflammasome overactivation. *ChinMed*. 2023;18(1):86. doi:10.1186/s13020-023-00800-1
37. Herb M, Schramm M. Functions of ROS in Macrophages and Antimicrobial Immunity. *Antioxidants*. 2021;10(2). doi:10.3390/antiox10020313
38. Wang Y, Zhu W, Lu D, Zhang C, Wang Y. Tetrahydropalmatine attenuates MSU crystal-induced gouty arthritis by inhibiting ROS-mediated NLRP3 inflammasome activation. *Int Immunopharmacol*. 2021;100:108107. doi:10.1016/j.intimp.2021.108107
39. Jiang T, Liu X, Wang S, et al. Paeoniflorin alleviated experimental Sjögren's syndrome by inhibiting NLRP3 inflammasome activation of submandibular gland cells via activating Nrf2/HO-1 pathway. *Free Radic Biol Med*. 2025;233:355–364. doi:10.1016/j.freeradbiomed.2025.03.043